Analysis of HSD3B7 knockout mice reveals that a 3α-hydroxyl stereochemistry is required for bile acid function

Heidi C. Shea*, Daphne D. Head*, Kenneth D. R. Setchell†, and David W. Russell*‡

*Department of Molecular Genetics, University of Texas Southwestern Medical Center, 5323 Harry Hines Boulevard, Dallas, TX 75390; and †Department of Pathology and Laboratory Medicine, Cincinnati Children's Hospital Medical Center, 3333 Burnet Avenue, Cincinnati, OH 45229

Primary bile acids are synthesized from cholesterol in the liver and thereafter are secreted into the bile and small intestine. Gut flora modify primary bile acids to produce secondary bile acids leading to a chemically diverse bile acid pool that is circulated between the small intestine and liver. A majority of primary and secondary bile acids in higher vertebrates have a 3α-hydroxyl group. Here, we characterize a line of knockout mice that cannot epimerize the 3β-hydroxyl group of cholesterol and as a consequence synthesize a bile acid pool in which 3β-hydroxylated bile acids predominate. This alteration causes death in 90% of newborn mice and decreases the absorption of dietary cholesterol in surviving adults. Negative feedback regulation of bile acid synthesis mediated by the farnesoid X receptor (FXR) is disrupted in the mutant mice. We conclude that the correct stereochemistry of a single hydroxyl group at carbon 3 in bile acids is required to maintain their physiologic and regulatory functions in mammals.

cholesterol turnover | lipid metabolism | liver disease | mouse model | nuclear receptor

Bile acids are required for normal digestion and absorption of lipids, and their synthesis by the liver represents the major pathway by which mammals catabolize cholesterol. The sequential actions of ≥16 enzymes in the pathway convert cholesterol, a molecule with a solubility of ≈10 nM in water (1), into a primary bile acid with a solubility that approaches ≈1.3 M (2). This enormous increase in solubility is affected by the addition of hydroxyl groups to the ring structure of the sterol and by the oxidation, shortening, and amidation of the side chain (3). These modifications in turn give bile acids amphiphilic properties that facilitate their transport from the liver into the bile by specific proteins located on apical membranes of hepatocytes (4).

After secretion into the bile, the conjugated primary bile acids synthesized in the liver follow an enterohepatic itinerary in which they are stored in the gallbladder, released into the duodenum of the small intestine in response to alimentary hormones, and thereafter progressively moved along the small bowel by peristalsis (5). Within the lumen of the gut, the amphiphilic properties of bile acids facilitate the formation of mixed micelles composed of dietary lipids, sterols, and fat-soluble vitamins, which once solubilized are absorbed by cells (enterocytes) that line the intestine. Upon reaching the distal small intestine, bile acids are taken up by specific transport proteins, moved across the enterocyte, and transferred into the portal vein for return to the liver (6). The enterohepatic cycle is completed by cell surface proteins on hepatocytes that transport bile acids from the portal circulation into the liver, from which they are again secreted into the bile (4). Within the gut, primary bile acids come in contact with bacterial flora that further modify their structures to produce dozens of secondary bile acids (7).

The uptake of bile acids from the terminal segment of the small intestine is generally an efficient process; however, a fraction of the bile acid pool escapes absorption and is lost in the feces each day. The lost bile acids, which amount to ≈0.5 g/day in humans and ≈0.05 g/day in mice (8), are replaced by the synthesis of new bile acids in the liver. The regulatory machinery that senses changes in the bile acid pool is located in the small intestine and liver and is composed of a network of genes activated by the transcription factor, farnesoid X receptor (FXR), a member of the nuclear receptor family (9). FXR is activated by binding bile acids; thus, the level of expression of FXR target genes is proportional to the size of the bile acid pool. In the small intestine, excess bile acids and FXR induce a fibroblast growth factor gene whose protein product acts as an endocrine hormone in the liver to repress bile acid synthesis (10). In the liver, activated FXR increases expression of short heterodimer partner (SHP), a transcriptional repressor of genes encoding the rate-limiting enzymes of bile acid synthesis (11, 12). Negative feedback inhibition is reversed by the aforementioned loss of bile acids from the pool, which reduces the activity of FXR and causes an increase in *de novo* bile acid synthesis.

The binding of bile acids by FXR is a crucial step in the initiation of negative feedback regulation. FXR is activated by some but not all bile acids (13–15). Structural studies show that the ligand binding pocket of FXR is composed of two sets of amino acids that interact with the amphiphilic bile acid. One set is made up of hydrophobic amino acids that interact with the hydrocarbon face of the bile acid, whereas the other set consists of hydrophilic residues that interact with the hydroxyl groups of the ligand (16, 17). This arrangement explains several prior observations concerning the ability of different bile acids to mediate feedback regulation. Although 17 of 19 carbons in the sterol nucleus are potential sites of hydroxylation, only five of these atoms (positions 3, 6, 7, 12, and 16) are hydroxylated in most species (18). In mammals, the stereochemistry of the hydroxyl groups at carbons 3, 7, and 12 is usually in the alpha configuration (19).

To investigate the roles of individual bile acids and their hydroxyl modifications in negative feedback regulation and nutrient absorption, we analyze mice with introduced mutations in select biosynthetic enzymes. In earlier studies, we found that inactivation of the sterol 12α-hydroxylase gene, which eliminates synthesis of 12α-hydroxylated bile acids, decreases the absorption of dietary cholesterol and derepresses bile acid synthesis in the liver (20). These findings reveal an essential role of the 12α-hydroxyl group in the

---

Fig. 1. Knockout of mouse *Hsd3b7*. (*A*) Schematic showing strategy used to delete *Hsd3b7*. Homologous recombination produced lines of ES cells in which *Hsd3b7* was replaced with the ''ACN'' cassette encoding neomycin resistance and Cre recombinase (24). Passage of the introduced mutation through the germ line resulted in deletion of the cassette, leaving behind a single LoxP site. (*B*) *Hsd3b7* genotyping of mice by PCR. Genomic DNA was extracted from mice of different *Hsd3b7* genotypes and subjected to amplification by PCR. The deduced genotype is shown above the agarose gel. M, size standards. (*C*) Detection of HSD3B7 by immunoblotting. Proteins extracted from human embryonic kidney 293 cells transfected with an HSD3B7 expression vector (293+), mock-transfected cells (293−), or from the livers of mice of the indicated *Hsd3b7* genotype (+/+, +/−, −/−) were separated by SDS/PAGE, transferred to nitrocellulose, and blotted with an antibody raised against a peptide antigen from the HSD3B7 enzyme. The positions to which proteins of known molecular weight migrated are shown at *Left*. Staining with Ponceau S revealed that similar amounts of protein were present in each lane of the blot.

solubilization of dietary sterols and in the activation of FXR in mice.

To gain insight into the role of the 3α-hydroxyl group in bile acid physiology, we here characterize a line of mice with a disruption in the gene encoding 3β-hydroxy-Δ^5-C$_{27}$-steroid oxidoreductase (HSD3B7). The HSD3B7 enzyme catalyzes two reactions required for the inversion of the 3β-hydroxyl group of cholesterol to the 3α-hydroxyl of bile acids. Mutations that inactivate this gene in humans cause a recessive form of neonatal liver failure (21–23). In the knockout mice, we find that elimination of HSD3B7 prevents epimerization of the hydroxyl group at carbon 3 of the sterol nucleus, resulting in the synthesis of 3β-hydroxylated bile acids. This stereochemical alteration eliminates cholesterol absorption in the gut and feedback regulation in the enterohepatic circulation. We conclude that the alpha stereochemistry of the 3-hydroxyl group conferred by HSD3B7 is required to maintain the functional and regulatory properties of bile acids in mice and presumably other species in which this modification is conserved.

Results

Construction of *Hsd3b7* Knockout Mice.
We took advantage of the small size of the mouse *Hsd3b7* (2.7 kb, six exons) to assemble a targeting vector that would allow complete replacement of the gene with a cassette encoding neomycin resistance after homologous recombination in ES cells (Fig. 1*A*). To ensure that the resulting phenotype was due to loss of *Hsd3b7* and not due to transcriptional interference from the neomycin resistance gene, the cassette was flanked by LoxP sites and contained a gene specifying Cre recombinase linked to a testis-specific promoter (24). Activation of the

Cre recombinase gene in germ cells of chimeric male mice was predicted to result in cassette excision, leaving behind a 34-bp LoxP site in place of *Hsd3b7* (Fig. 1*A*).

Homologous recombination in ES cells occurred at a high frequency (40%) after introduction of the targeting vector, and six independently derived ES cell clones produced chimeric animals that transmitted the altered *Hsd3b7* through the germline. The mutant allele was inherited in Mendelian fashion (Fig. 1*B*), and expected numbers of wild-type, heterozygous, and homozygous offspring were born. Equal numbers of male and female pups were obtained in crosses between heterozygous carriers of the mutant gene. Fertility and fecundity were normal in mice heterozygous and homozygous for the introduced mutation.

The effects of the mutation on the expression of HSD3B7 mRNA and protein in the liver were determined by real time RT-PCR and immunoblotting. Abundant HSD3B7 mRNA was detected in the livers of wild-type mice; levels of this mRNA were reduced by half in heterozygous mice and to undetectable levels in homozygous mice (data not shown). As judged by SDS/PAGE and immunoblotting (Fig. 1*C*), the normal HSD3B7 protein migrated with an apparent molecular weight of ≈33,000. The amount of this protein was reduced by half in mice heterozygous for the disrupted gene and was undetectable in animals homozygous for the mutant allele.

Phenotype of *Hsd3b7*−/− Mice.
Mice lacking HSD3B7 were outwardly normal at birth, but a majority failed to grow at a normal rate and died within the first 18 days of postnatal life when maintained on standard laboratory chow and water (Fig. 2*A*). Death occurred in two waves, with ≈45% of homozygous male and female animals dying in the first 4 days of life and another ≈45% dying between days 8 and 18. Only a few animals survived beyond weaning (postnatal day 21). Addition of a pan-vitamin supplement to the drinking water and a bile acid (0.1% cholic acid) to the diet during late gestation and continuing through postnatal day 28 resulted in an approximate doubling of the survival frequency. When the level of dietary bile acid was increased to 0.5% and vitamin supplementation was maintained, survival of the mutant mice approached that of wild-type mice (Fig. 2*A*), The fur of *Hsd3b7*−/− suckling mice and nursing mothers maintained on unsupplemented chow and water was oily (Fig. 2*B*), and the skin was scaly (Fig. 2*C*). These traits were not observed in wild-type mice or those heterozygous for the introduced mutation. Vitamin and bile acid supplementation prevented the appearance of these features in homozygous mice.

Adult *Hsd3b7*−/− animals maintained on vitamin and bile acid supplements through postnatal day 28 and thereafter switched to normal laboratory chow attained body weights similar to those of wild-type controls (Table 1). There was no apparent organomegaly in tissues of the enterohepatic circulation, and plasma cholesterol levels were normal. Kidney and liver cholesterol levels were not significantly different. A 32% decrease in plasma triglycerides was measured together with a 30% increase in hepatic triglyceride levels (Table 1). Liver histology of knockout animals up to 1.5 years of age was normal, and in agreement with this finding, the liver enzymes aspartate aminotransferase and alanine aminotransferase were not elevated in the plasma.

Sterol and Bile Acid Metabolism in *Hsd3b7*−/− Mice.
Bile acid pool size was determined by HPLC and found to be decreased by ≈33% in HSD3b7−/− vs. control mice, a difference that was not statistically significant (Fig. 3*A*). Rates of fecal bile acid excretion determined by HPLC analysis of bile acids in the stool were increased ≈2-fold in the knockout mice (Fig. 3*B*). Fecal neutral sterols also were excreted at a rate that was 2.8-fold higher in knockout mice than in wild-type littermates (Fig. 3*C*), and, consistent with this increase in sterol loss, intestinal cholesterol absorption was decreased to <9% of normal in *Hsd3b7*−/− mice (Fig. 3*D*).

We next measured rates of cholesterol synthesis in the tissues of wild-type and knockout mice, using a [^{3}H]H$_2$O incorporation assay
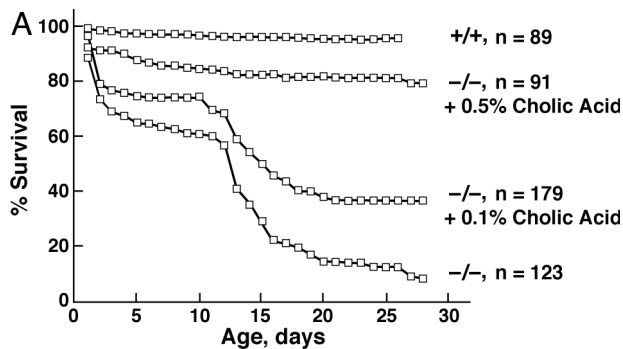
Fig. 2. Phenotype of Hsd3b7⁻/⁻ mice. (A) Survival curves depicting frequency of death in wild-type mice (+/+) and homozygous Hsd3b7 knockout mice (−/−). Addition of a pan-vitamin supplement to the drinking water and increasing amounts of cholic acid to the diet increased survival of the mutant mice. Sample size (n) ranged from 89 to 179 mice of the indicated genotypes and included both sexes. (B) Oily appearance of fur in young Hsd3b7⁻/⁻ mice. A wild-type animal with normal, healthy fur is shown at *Left*, and an age-matched knockout animal with oily fur and microsomia is shown at *Right*. (C) Scaly appearance of skin in young Hsd3b7⁻/⁻ mice. A runted knockout mouse is shown at *Right* with scales on the skin of the forelegs and at the caudal end of the body. A normal littermate is shown at *Left*.

(25). As indicated by the data in Fig. 4A, elimination of Hsd3b7 caused a 3.5-fold increase in *de novo* cholesterol synthesis in the liver and smaller but significant increases in the duodenal and jejunal segments of the small intestine. In contrast to these results, cholesterol synthesis rates were not changed in the terminal segment (ileum) of the small intestine or in the spleen. A modest but significant decrease in cholesterol synthesis was detected in the kidney. These findings suggested that Hsd3b7⁻/⁻ mice compensated for the loss of dietary cholesterol (Fig. 3D) by increasing rates

Table 1. Physical and physiologic characteristics of Hsd3b7⁺/⁺ and Hsd3b7⁻/⁻ mice

|	Genotype	
Parameter	Hsd3b7⁺/⁺	Hsd3b7⁻/⁻
Animal weight, g	26.3 ± 0.7 (13)	26.2 ± 0.9 (18)
Liver weight, g	1.5 ± 0.1 (6)	1.5 ± 0.6 (6)
Small intestine weight, g	1.2 ± 0.5 (6)	1.4 ± 0.1 (6)
Plasma cholesterol, mg/dl	99.7 ± 6.8 (6)	97 ± 7.2 (6)
Plasma triglyceride, mg/dl	94.5 ± 7.7 (6)	64.6 ± 6.2 (6)*
Liver cholesterol, mg/g	2.5 ± 0.06 (11)	2.3 ± 0.06 (11)
Liver triglyceride, mg/g	10.0 ± 1.0 (11)	13.0 ± 1.0 (11)*
Kidney cholesterol, mg/g	4.0 ± 0.2 (6)	3.7 ± 0.1 (6)

Wild-type and knockout male mice were maintained on vitamin and bile acid supplements through postnatal day 28 and thereafter on normal laboratory chow containing 4% (wt/wt) fat diet and then studied at 3–4 months of age. Values shown are means ± 1 SE derived from the number of mice given in parentheses.
*Statistically different from value for Hsd3b7⁺/⁺ group (P < 0.05).
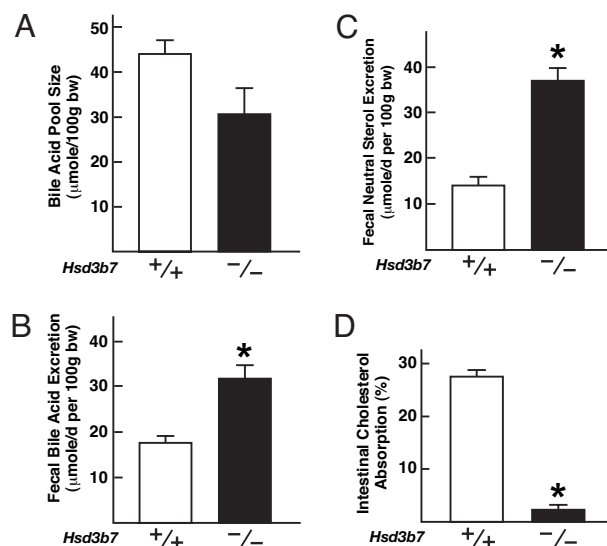
Fig. 3. Bile acid and sterol metabolism in wild-type and Hsd3b7⁻/⁻ mice. (A) Bile acid pool sizes were determined by HPLC analysis. The reduction in pool size observed in the knockout mice did not reach statistical significance. (B) Rates of fecal bile acid excretion were determined by HPLC analysis and were significantly different (*, P < 0.05) in mice of different Hsd3b7 genotypes. (C) Fecal neutral sterol excretion rates were determined by GC. Hsd3b7⁻/⁻ mice excreted 2.8-fold more neutral sterols than did wild-type mice. (D) Intestinal cholesterol absorption was determined by using a fecal dual-isotope ratio method and found to be significantly reduced in the mutant mice. All experiments shown in A–D were repeated a minimum of two times with different animals (n = 5–6 animals per genotype) on different days.

of *de novo* cholesterol synthesis in the liver and initial segments of the gut (Fig. 4A). Rates of fatty acid synthesis increased ≈20% in the livers of knockout mice but were unchanged in the other tissues examined (Fig. 4B).
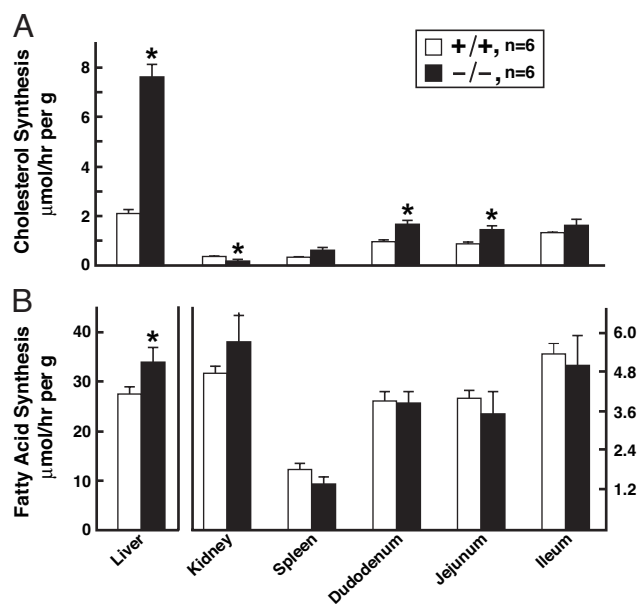
Fig. 4. Rates of *de novo* cholesterol and fatty acid synthesis in wild-type and knockout mice. Sterol (A) and fatty acid (B) synthesis were measured *in vivo* in the indicated tissues of six Hsd3b7⁺/⁺ and six Hsd3b7⁻/⁻ mice, using a [³H₂O] incorporation assay. Values, which represent means 1 ± SE, marked with an asterisk were significantly different from those in the Hsd3b7⁺/⁺ mice. Similar results were obtained in a second independent experiment.
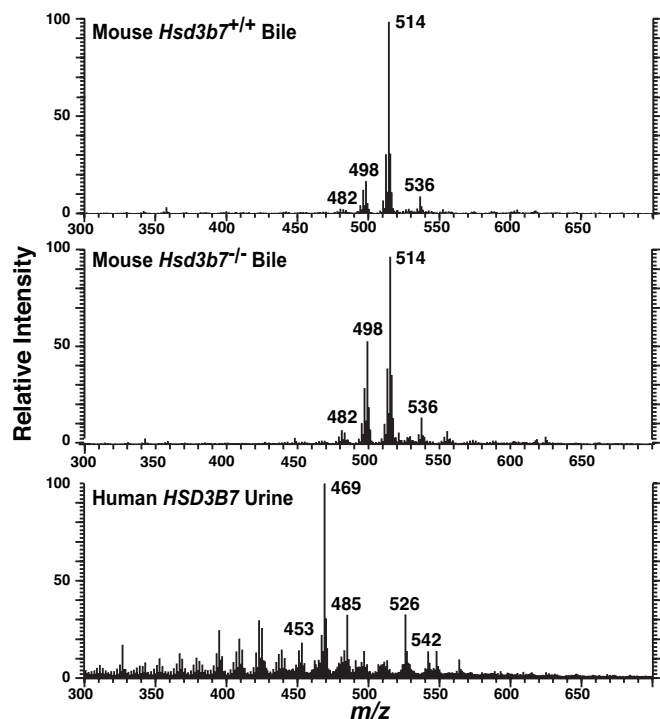
Fig. 5. Negative ion FAB-MS analyses of bile from $Hsd3b7^{+/+}$ and $Hsd3b7^{-/-}$ mice and urine from a human subject with $HSD3B7$ deficiency. Bile was collected from the gallbladders of mice of the indicated $Hsd3b7$ genotypes that had been fasted for 4 h. Bile acids were extracted into methanol, and the equivalent of 1 μl of bile was analyzed directly by FAB-MS. Negative ion spectra were recorded over the mass range (m/z) 50–800 Da. The major ions observed in the bile of wild-type and knockout animals (m/z 514 and 498) were similar and represented typical mouse dihydroxy- and trihydroxy-cholanoic acids. The spectrum of a urine sample from a human patient with $HSD3B7$ deficiency is shown in *Bottom*. Two diagnostic ion pairs were observed at m/z 469 and 485, and m/z 526 and 542, which represented the sulfated and glyco-sulfated metabolites of $3\beta,7\alpha$-dihydroxy-5-cholen-24-oic and $3\beta,7\alpha,12\alpha$-trihydroxy-5-cholen-24-oic acids, respectively.

Fast Atom Bombardment (FAB)-MS Analyses of Bile Acids in $Hsd3b7^{-/-}$ Mice. The presence of an insignificantly different bile acid pool size in the mutant mice together with an increased rate of bile acid and fecal neutral sterol excretion and decreased cholesterol absorption suggested that the composition of the bile acid pool was different in these animals. To test this hypothesis, we first used FAB-MS, which is routinely used to diagnose the presence of $HSD3B7$ deficiency in human subjects (26). As shown in Fig. 5, the negative ion FAB-MS mass spectra obtained from bile pooled from wild-type and knockout mice were virtually identical and contained major ions at m/z 514 and 498 representing the taurine conjugates of typical mouse dihydroxy- and trihydroxy-cholanoic acids. These data were consistent with the presence of primary bile acids in mice of both $Hsd3b7$ genotypes and with the fact that the mouse is an obligate taurine conjugator. No bile acids were detected by FAB-MS analyses of urine samples from wild-type and null mice (data not shown).

For comparison, we acquired the spectrum of a urine sample from a human patient with $HSD3B7$ deficiency (Fig. 5). As expected, two specific pairs of ions were observed at m/z 469 and 485, and m/z 526 and 542, which represented the sulfated and glyco-sulfated metabolites of $3\beta,7\alpha$-dihydroxy-5-cholen-24-oic and $3\beta,7\alpha,12\alpha$-trihydroxy-5-cholen-24-oic acids, respectively, that accumulate in subjects with this genetic disease. The absence of these or related 3β-hydroxy-Δ^5 bile acids in bile and urine of adult HSD3B7

knockout mice suggested the presence of a compensatory metabolic pathway that prevented their accumulation.

GC-MS Analyses of Bile Acids in $Hsd3b7^{-/-}$ Mice. We next carried out GC-MS analyses of bile acids present in gallbladder bile of wild-type and knockout animals. As expected, the bile of wild-type mice contained three major bile acids corresponding to cholic acid ($3\alpha,7\alpha,12\alpha$-trihydroxy-5β-cholanoic acid), β-muricholic acid ($3\alpha,6\beta,7\beta$-trihydroxy-5β-cholanoic acid), and ω-muricholic acid ($3\alpha,6\alpha,7\beta$-trihydroxy-5β-cholanoic acid) (Fig. 6A). The bile of knockout mice contained these three bile acids and two additional major species that eluted from the GC column on both sides of cholic acid, and several minor species (Fig. 6A). The mass spectrum of the bile acid eluting just before cholic acid suggested the presence of a trihydroxy-cholanoate structure (Fig. 6B, scan 265). The molecular ion, of low intensity, was at m/z 638, and the ion sequence of three losses of trimethylsilanol (TMS), yielding m/z 548 (M-90), m/z 458 (M-[2 × 90]), and m/z 368 (M-[3 × 90]), together with the loss of the side chain (-115 Da) to give rise to the ABCD-ring fragment at m/z 253, established a trihydroxylated C-24 bile acid. The relative intensities of these ions differentiated two possible stereoisomers of a 3,7,12-trihydroxy bile acid; the intense ion at m/z 343 representing the loss of two TMS groups and the side chain was more abundant in the $3\beta,7\alpha,12\alpha$-trihydroxy-5β-cholanoic acid stereoisomer (Fig. 6B, scan 265, arrow) than it was in the $3\alpha,7\alpha,12\alpha$-trihydroxy-5β-cholanoic acid stereoisomer (Fig. 6B, scan 278).

The mass spectrum of the bile acid eluting just after cholic acid suggested the presence of a dihydroxy-cholanoate structure (Fig. 6B, scan 286). The molecular ion was at m/z 550 consistent with a dihydroxy C-24 bile acid. Sequential losses of two TMS groups gave rise to ions at m/z 460 and 370, followed by the loss of the side chain (-115 Da) to account for the ABCD-ring fragment at m/z 255. The ion at m/z 405 in this spectrum, which is accounted for by loss of carbon atoms C-1 to C-4 of the A-ring, was diagnostic of a 3,6-dihydroxy-bile acid vs. a 3,7- or a 3,12-dihydroxylated bile acid. The ion at m/z 323 is also prominent in 3,6-dihydroxy bile acids, being formed by cleavage across the B- and C-rings. From these data and the retention index of the peak, we deduced that this species represented the methyl ester-TMS ether derivative of $3\beta,6\alpha$-dihydroxy-5β-cholanoic acid. For comparison, the mass spectrum of the major trihydroxylated 6β-hydroxy bile acid, β-muricholic acid, is shown in Fig. 6B, scan 337.

Supporting information (SI) Table 2 summarizes the individual bile acids detected and their concentrations in pooled gallbladder bile samples from wild-type and knockout mice, which were determined as described in *SI Materials and Methods*. Together, these MS analyses indicated that $Hsd3b7^{-/-}$ mice contained reduced amounts of normal bile acids and two additional atypical bile acids, $3\beta,7\alpha,12\alpha$-trihydroxy-5β-cholanoic acid and $3\beta,6\alpha$-dihydroxy-5β-cholanoic acid.

Gene Expression in $Hsd3b7^{-/-}$ Mice. To determine the regulatory effects of the altered bile acid pool composition in $Hsd3b7^{-/-}$ mice, we used real-time RT-PCR to assess mRNA levels in tissues of the enterohepatic circulation. As shown by the data in Fig. 7A, the amounts of cholesterol 7α-hydroxylase and sterol 12α-hydroxylase mRNAs, which are normally repressed by bile acids acting through FXR, were elevated 4-fold compared with those of wild-type mice. As a control, the sterol 27-hydroxylase mRNA level, which does not respond to bile acids, was unchanged in the knockout mice. Unexpectedly, the levels of two other normally constitutively expressed mRNAs, encoding the bile acid biosynthetic enzyme steroid 5β-reductase and racemase, were increased $\approx$3-fold in the mutant mice. SHP mRNA levels, which are normally induced by FXR and bile acids, were decreased $\approx$2-fold in $Hsd3b7^{-/-}$ livers. The increased rate of cholesterol synthesis reported in Fig. 4A, was reflected by an elevation in the level of mRNA encoding the
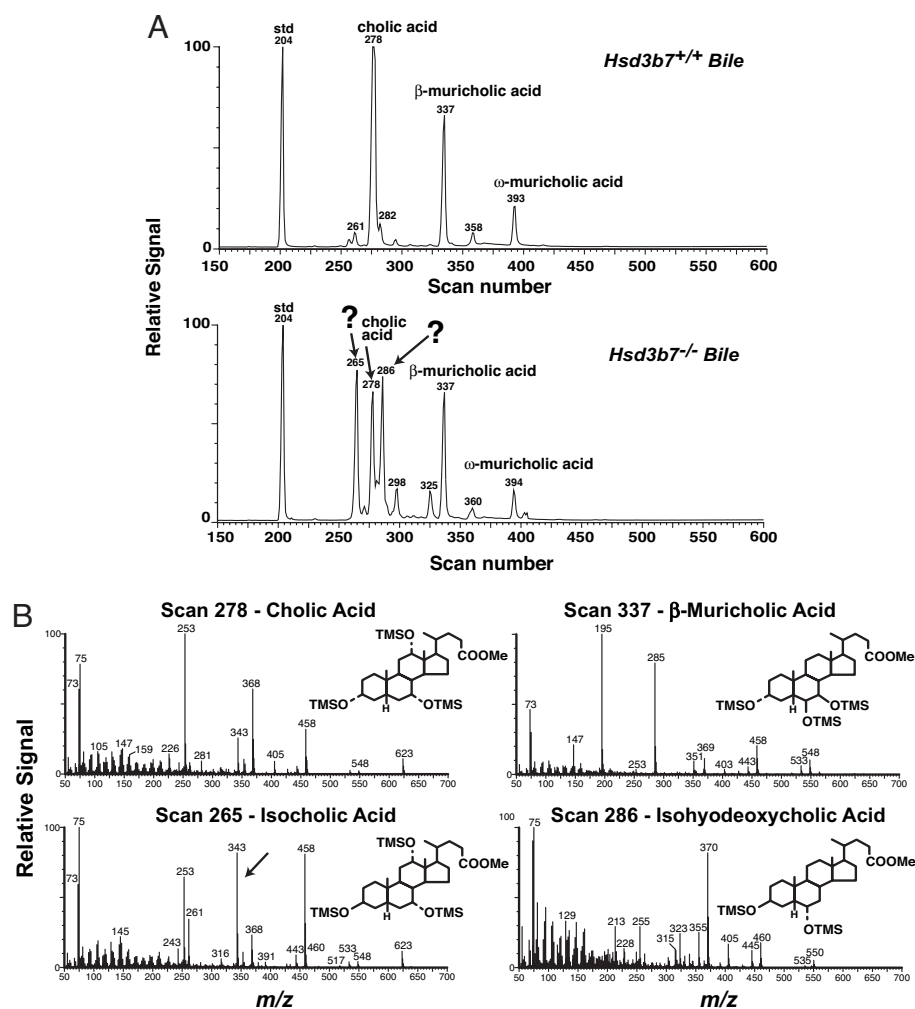
Fig. 6. GC-MS analyses of gallbladder bile acids in *Hsd3b7*^{+/+} and *Hsd3b7*^{−/−} mice. (*A*) Total ion chromatograms from GC-MS analyses of the methyl ester-TMS derivatives isolated after solvolysis and hydrolysis of bile acids in the gallbladder bile of wild-type (*Upper*) and knockout (*Lower*) mice. Major peaks were identified by comparison of retention times to those of authentic standards. *std*, elution position of internal standard, nordeoxycholic acid. (*B*) Electron ionization (70 eV) mass spectra of the major known and unknown compounds identified in the gallbladder bile of wild-type and knockout mice. The chemical structures deduced from the impact spectra are shown in the upper right of individual panels.

rate-limiting enzyme in this pathway, hydroxymethylglutaryl CoA reductase, whereas increases in mRNAs encoding acetyl-CoA carboxylase 1, fatty acid synthase, and stearoyl-CoA desaturase 1 mirrored the enhanced rates of fatty acid synthesis measured in these animals. The changes observed in these mRNA levels were confirmed by microarray hybridization (data not shown) and, in the case of cholesterol 7α-hydroxylase, at the protein level by immunoblotting (Fig. 7*A Inset*).

In the gut, the alteration in bile acid pool composition led to a decrease in the levels of two known FXR target mRNAs, those specifying SHP and fibroblast growth factor 15 (Fig. 7*B*). The increased rate of cholesterol synthesis was paralleled by an elevation in the amount of hydroxymethylglutaryl CoA reductase mRNA.

Discussion

The current data indicate that loss of the HSD3B7 enzyme in the mouse changes the types of bile acids synthesized by the liver. Instead of the normal complement of 3α-hydroxylated bile acids, *Hsd3b7*^{−/−} mice produce large quantities of stereoisomeric 3β-hydroxylated bile acids that have different physiochemical properties. 3β-Hydroxylated-bile acids are less efficient at solubilizing essential nutrients from the diet, leading to death in the postnatal period and to a reduction in the amount of dietary

cholesterol absorbed by adult mice. Similarly, mice with a preponderance of 3β-hydroxylated bile acids do not activate feedback repression of bile acid synthesis, leading to derepression of two rate-limiting enzymes in the pathway. Together, these findings underscore the importance of a 3α-hydroxyl stereochemistry for proper bile acid function and regulation.

The biphasic death curve observed in *Hsd3b7*^{−/−} mice fed normal chow is the same as that seen in mice lacking cholesterol 7α-hydroxylase (27), the enzyme that initiates the classic pathway of bile acid synthesis. Death in the 7α-hydroxylase-deficient animals was initially attributed to the absence of bile acid synthesis during early life; however, subsequent chemical analysis of bile acids in neonates showed an accumulation of two monohydroxylated bile acids, which were postulated to be hepatotoxic and the causative agents of death (28). One of these two atypical bile acids, 3β-hydroxy-5-cholenoate, had a 3β-hydroxyl stereochemistry like those detected in the adult *Hsd3b7*^{−/−} mice studied here. It is thus possible that a combination of nutrient deprivation and hepatotoxicity associated with 3β-hydroxyl bile acids cause death in newborn *Hsd3b7*^{−/−} mice.

The two predominant 3β-hydroxylated bile acids detected in the *Hsd3b7*^{−/−} mice, 3β,7α,12α-trihydroxy-5β-cholanoic acid and 3β,6α-dihydroxy-5β-cholanoic acid (Fig. 6), have not been reported
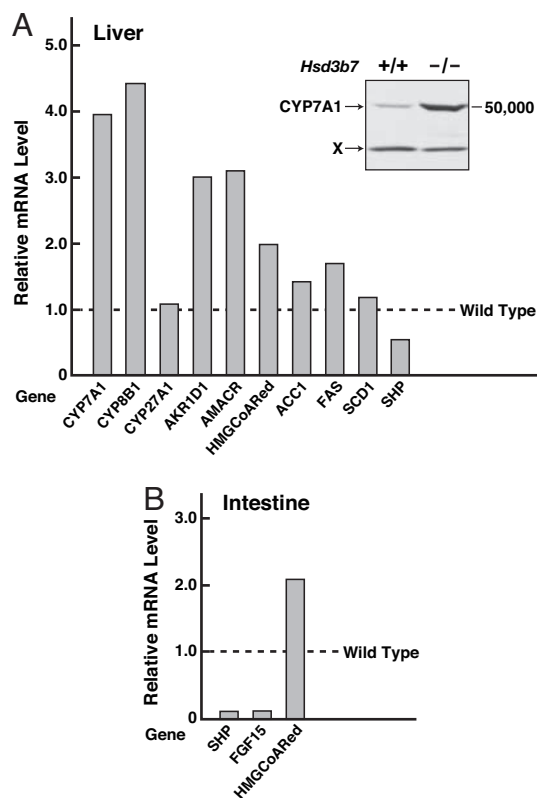
Fig. 7. Real-time RT-PCR analysis of RNAs isolated from liver (*A*) and intestine (*B*) of $Hsd3b7^{+/+}$ and $Hsd3b7^{-/-}$ mice. The level of each mRNA in the wild-type tissue was set to one. *CYP8B1*, sterol 12α-hydroxylase; *CYP27A1*, sterol 27-hydroxylase; *AKR1D1*, steroid 5β-reductase; *AMACR*, α-methylacyl CoA racemase; HMGCoARed, hydroxymethylglutaryl CoA reductase; ACC1, acetyl-CoA carboxylase 1; FAS, fatty acid synthase; SCD1, stearoyl CoA desaturase 1; FGF15, fibroblast growth factor 15. An immunoblot of hepatic membrane proteins isolated from mice of the indicated *Hsd3b7* genotypes and probed with an antiserum directed against the cholesterol 7α-hydroxylase (CYP7A1) protein is shown in *Inset*. x, cross-reacting protein.

in this species. The first is a stereoisomer of cholic acid, a normally abundant bile acid in the mouse, whereas the second is a stereoisomer of hyodeoxycholic acid, which is not found in normal mouse bile but is a predominant bile acid in adult knockout mice lacking cholesterol 7α-hydroxylase (29). In the synthesis of 3α-hydroxylated bile acids, HSD3B7 catalyzes the isomerization of the Δ^5 double bond to the Δ^4 position and the oxidation of the 3β-hydroxyl group to a 3-oxo group. The steroid 5β-reductase enzyme then reduces the Δ^4 bond and a 3α-hydroxysteroid dehydrogenase enzyme reduces the 3-oxo group to produce a 3α-hydroxylated intermediate of bile acid synthesis. The absence of desaturation in the A or B rings of the 3β-hydroxylated bile acids detected in $Hsd3b7^{-/-}$ mice suggests the existence of a compensatory enzyme that catalyzes reduction of the Δ^5 bond without affecting the 3β-hydroxyl group. We do not know whether this reaction is carried out by a hepatic isomerase that moves the double bond from the B to the A ring of the sterol to allow subsequent reduction by the steroid 5β-reductase, or by an enzyme system present in the gut flora. The latter possibility is suggested by earlier studies done in rabbits, humans, and bacteria on the origin of 3β-hydroxylated bile acids (30, 31) and by the bile acid composition of human ceca (32). It also is feasible that the increased levels of steroid 5β-reductase detected in the knockout mice (Fig. 7*A*), act directly on Δ^5, 3β-hydroxyl intermediates to produce a saturated B-ring.

3β-Hydroxylated bile acids are efficiently epimerized to their 3α-hydroxylated forms after infusion into rats (33, 34), after incu-

bation with purified human liver enzymes (35, 36), and after oral administration to humans (37). A similar biosynthetic origin may explain the reduced amounts of 3α-hydroxylated bile acids detected in the $Hsd3b7^{-/-}$ mice.

Alterations in the size and composition of the bile acid pool in mice affect the absorption of nutrients by the small intestine and the regulation of gene expression in this tissue and the liver (20, 38). With respect to absorption, 3β-hydroxylated bile acids have higher critical micellization concentrations than their 3α-hydroxylated counterparts (39). For example, the critical micellization concentration of isocholic acid is 90 mM in H_2O vs. 13 mM for cholic acid. The presence of 3β-hydroxylated bile acids in the $Hsd3b7^{-/-}$ mice would thus lead to decreased solubilization of fat-soluble vitamins and cholesterol (Fig. 3*D*) and perhaps to interference with the solubilization of these nutrients by the small amounts of 3α-hydroxylated bile acids that are present.

Feedback regulation of bile acid synthesis is mediated by the binding of excess bile acids to the nuclear receptor FXR, which then activates a network of genes involved in controlling synthesis (9). The loss of feedback regulation in $Hsd3b7^{-/-}$ mice implies that the excess 3β-hydroxylated bile acids in these animals must in some manner interfere with FXR action. These atypical bile acids may act as antagonists of 3α-hydroxylated bile acids by competing for binding to FXR, or they may decrease the uptake of normal bile acids, thereby preventing their intracellular access to FXR. The latter explanation is favored by the observation that approximately two times more bile acids are lost to the stool in knockout vs. wild-type mice (Fig. 3*B*), and by the measurement of ileal absorption rates of 3α- vs. 3β-hydroxylated bile acids (34). Future studies in whole animals, primary hepatocytes, and transfected cells may reveal additional insight into the mechanisms by which 3β-hydroxylated bile acids alter feedback regulation.

Materials and Methods

Construction of Targeting Vector. A plasmid vector designed to delete the six exons of *Hsd3b7* by homologous recombination in mouse ES cells was constructed by using standard methods (40), the vector pPolIIshort-neobPA-HSVTK (41), and the "ACN cassette" (24).

ES Cell Culture. Mouse I1C ES cells derived from the 129SvEv strain were used in homologous recombination experiments as described in ref. 20. The frequency of ES cell clones that underwent homologous recombination was 40% (132/384 screened). Injection of four of these clones into C57BL/6J blastocysts produced 24 chimeric males that had contributions from the ES cells ranging from 50% to 80% based on the amount of agouti coat color. Of these mice, six transmitted the disrupted gene through the germline. Experiments reported here were performed in mice of mixed strain (C57BL/6J-129SvEv) descendants (F_2 and subsequent generations) of these animals. No phenotypic differences were observed between knockout mice derived from two independent ES cell clones.

PCR Genotyping. Routine genotyping of mice was performed on genomic DNA extracted from tails (DirectPCR lysis reagents; Viagen Biotech, Los Angeles, CA), using three oligonucleotide primers in a multiplex PCR. The oligonucleotides used were: wild-type allele 5′ primer, GCCACAGTGGGTGAAGCAGG; targeted allele 5′ primer, AAGGACAGAACCTGCCCATTT-GGT; and common 3′ primer, GGTAGCTGAAGTAAGCA-GACCAGC.

Animals and Diets. Animals were housed in cages containing wood shavings in a temperature-controlled room (22°C) with 12-hr light/dark cycling. All experiments were performed toward the end of the 12-hr dark phase of the cycle, and all mice were in the fed state at the time of study unless otherwise stated. Experiments were

BIOCHEMISTRY

approved by the University of Texas Southwestern Institutional Animal Care and Research Advisory Committee.

Survival studies used a cereal-based rodent diet, Teklad 7002 (Harlan Teklad, Madison, WI), which contained 6% (wt/wt) fat, 24% (wt/wt) protein, and 5% (wt/wt) fiber. To increase survival of $Hsd3b7^{-/-}$ pups, pregnant and nursing mothers were provided water supplemented with vitamins (CritterVites; Mardel, Glendale Heights, IL) and fed Teklad 7002 supplemented with either 0.1% (wt/wt) or 0.5% cholic acid (catalog nos. TD03626 and TD04046, respectively; Harlan Teklad). These supplements were begun on gestation day 12 and continued until the fourth postnatal week, at which time the animals were fed Teklad 7001 (Harlan Teklad), which contained 4% (wt/wt) fat, 24% (wt/wt) protein, and 5% (wt/wt) fiber. To ensure complete purging of cholic acid provided as a supplement to newborn and juvenile $Hsd3b7^{-/-}$ mice, animals in which bile acid pool size and composition were determined were fed the unsupplemented Teklad 7001 diet a minimum of 2 months before study.

Intestinal Cholesterol Absorption. Cholesterol absorption was measured by a fecal dual-isotope ratio method (42).

Bile Acid Composition and Pool Size. Bile acids were isolated from the gallbladder, surrounding liver tissue, and small intestine of individual mice by extraction into ethanol with [24-^{14}C]taurocholic acid (New England Nuclear, Waltham, MA) added as an internal standard. Individual bile acids were resolved and quantitated after HPLC on a Hewlett Packard (Palo Alto, CA) series 1100 system with refractive index detector (38).

Fecal Bile Acid and Neutral Sterol Excretion. Mice were singly housed in fresh cages for 3 days, and their feces were collected and extracted as described in refs. 20 and 38.

Cholesterol and Fatty Acid Synthesis. Rates of *de novo* sterol and fatty acid synthesis were measured by using a [^{3}H]H$_2$O incorporation assay (25).

Plasma and Tissue Lipid Levels. Mice were exsanguinated from the vena cava under isoflurane anesthesia. Cholesterol and triglyceride levels were determined in plasma and 100-mg aliquots of frozen liver from knockout and wild-type mice, using commercially available kits (Chol 1127771; Roche Diagnostics, Nutley, NJ; and Infinity; Thermo Electron, Melbourne, Australia) (43).

RNA and Protein Blotting. Total RNA was extracted from liver and small intestine, using RNA Stat-60 kits (Tel-Test B, Friendswood, TX). For real time RT-PCR, equal amounts of RNA isolated from individual mice were pooled, and cDNA derived from 20 ng of total RNA was used in each reaction.

Protein extracts were prepared by homogenizing freshly harvested livers in 0.25 M sucrose buffer [0.25 M sucrose/20 mM Tris-acetate, pH 7.4/1 mM EDTA and one tablet of an EDTA-free protease inhibitor mixture tablet per 7 ml of buffer (Roche Diagnostics, Mannheim, Germany)], using a polytron, followed by centrifugation at $600 \times g$ for 10 min. Membranes were prepared by subjecting the supernatant to an additional centrifugation at $100,000 \times g$ for 30 min at 4°C. The resulting pellets were resuspended in 50 mM Tris·acetate, pH 7.4/1 mM EDTA/20% (vol/vol) glycerol, and protease inhibitor as described above. A rabbit polyclonal antibody that recognizes amino acids 340–354 of the mouse HSD3B7 was used to detect protein expression (22). Cholesterol 7α-hydroxylase and sterol 27-hydroxylase proteins were identified by using rabbit polyclonal antisera (44).

FAB Mass Spectrometry (FAB-MS). Bile was collected from the gallbladders of mice fasted for 4 h. Bile acids were analyzed directly with no prior work-up of the sample. Negative ion FAB-MS spectra were recorded after placing the equivalent of 1 μl of bile onto a small drop of glycerol spotted on the target probe. The probe was introduced into the ion source of an Autospec Q magnetic sector mass spectrometer, and a beam of fast atoms of cesium was fired at the target. Negative ion spectra (scan time 1.5 sec) were recorded over the mass range (m/z) 50–800 Da and compared with those of known bile acid conjugates and biosynthetic intermediates (45, 46).

1. Renshaw PF, Janoff AS, Miller KW (1983) *J Lipid Res* 24:47–51.
2. Small DM, Bourges M, Dervichian DG (1966) *Nature* 211:816–818.
3. Russell DW (2003) *Annu Rev Biochem* 72:137–174.
4. Borst P, Elferink RO (2002) *Annu Rev Biochem* 71:537–592.
5. Carey MC (1982) in *The Liver, Biology and Pathobiology* (Raven, New York), pp 429–465.
6. Love MW, Dawson PA (1998) *Curr Opin Lipidol* 9:225–229.
7. Hylemon PB, Harder J (1998) *FEMS Microbiol Rev* 22:475–488.
8. Dietschy JM, Turley SD (2002) *J Biol Chem* 277:3801–3804.
9. Kalaany NY, Mangelsdorf DJ (2006) *Annu Rev Physiol* 68:159–191.
10. Inagaki T, Choi M, Moschetta A, Peng L, Cummins CL, McDonald JG, Luo G, Jones SA, Goodwin B, Richardson JA, *et al.* (2005) *Cell Metab* 2:217–225.
11. Goodwin B, Jones SA, Price RR, Watson MA, McKee DD, Moore LB, Galardi C, Wilson JG, Lewis MC, Roth ME, *et al.* (2000) *Mol Cell* 6:517–526.
12. Lu TT, Makishima M, Repa JJ, Schoonjans K, Kerr TA, Auwerx J, Mangelsdorf DJ (2000) *Mol Cell* 6:507–515.
13. Makishima M, Okamoto AY, Repa JJ, Tu H, Learned RM, Luk A, Hull MV, Lustig KD, Mangelsdorf DJ, Shan B (1999) *Science* 284:1362–1365.
14. Parks DJ, Blanchard SG, Bledsoe RK, Chandra G, Consler TG, Kliewer SA, Stimmel JB, Willson TM, Zavacki AM, Moore DD, *et al.* (1999) *Science* 284:1365–1368.
15. Wang H, Chen J, Hollister K, Sowers LC, Forman BM (1999) *Mol Cell* 3:543–553.
16. Downes M, Verdecia MA, Roecker AJ, Hughes R, Hogenesch JB, Kast-Woelbern HR, Bowman ME, Ferrer JL, Anisfeld AM, Edwards PA, *et al.* (2003) *Mol Cell* 11:1079–1092.
17. Mi L-Z, Devarakonda S, Harp JM, Han Q, Pellicciari R, Willson TM, Khorasanizadeh S, Rastinejad F (2003) *Mol Cell* 11:1093–1100.
18. Haslewood GAD (1967) *J Lipid Res* 8:535–550.
19. Matschiner JT (1971) in *The Bile Acids, Chemistry, Physiology, and Metabolism*, eds Nair PP, Kritchevsky D (Plenum, New York), pp 11–46.
20. Li-Hawkins J, Gafvels M, Olin M, Lund EG, Andersson U, Schuster G, Bjorkhem I, Russell DW, Eggertsen G (2002) *J Clin Invest* 110:1191–1200.
21. Clayton PT, Leonard JV, Lawson AM, Setchell KD, Andersson S, Egestad B, Sjovall J (1987) *J Clin Invest* 79:1031–1038.
22. Schwarz M, Wright AC, Davis DL, Nazer H, Bjorkhem I, Russell DW (2000) *J Clin Invest* 106:1175–1184.
23. Cheng JB, Jacquemin E, Gerhardt M, Nazer H, Cresteil D, Heubi JE, Setchell KDR, Russell DW (2003) *J Clin Endocrinol Metab* 88:1833–1841.
24. Bunting M, Bernstein KE, Greer JM, Capecchi MR, Thomas KR (1999) *Genes Dev* 13:1524–1528.
25. Dietschy JM, Spady DK (1984) *J Lipid Res* 25:1469–1476.
26. Jacquemin E, Setchell KD, O'Connell NC, Estrada A, Maggiore G, Schmitz J, Hadchouel M, Bernard O (1994) *J Pediatr* 125:379–384.
27. Ishibashi S, Schwarz M, Frykman PK, Herz J, Russell DW (1996) *J Biol Chem* 271:18017–18023.
28. Arnon R, Yoshimura T, Reiss A, Budai K, Lefkowitch JH, Javitt NB (1998) *Gastroenterology* 115:1223–1228.
29. Schwarz M, Lund EG, Setchell KDR, Kayden HJ, Zerwekh JE, Bjorkhem I, Herz J, Russell DW (1996) *J Biol Chem* 271:18024–18031.
30. Heftmann E, Weiss E, Miller HK, Mosettig E (1959) *Arch Biochem Biophys* 84:324–341.
31. Danielsson H, Eneroth P, Hellstrom K, Sjovall J (1962) *J Biol Chem* 237:3657–3659.
32. Hamilton JP, Xie G, Raufman JP, Hogan S, Griffin TL, Packard CA, Chatfield DA, Hagey LR, Steinbach JH, Hofmann AF (2007) *Am J Physiol*, 10.1152/ajpgi.00027.2007.
33. Shefer S, Salen G, Hauser S, Dayal B, Batta AK (1981) *J Biol Chem* 257:1401–1406.

34. Marcus SN, Schteingart CD, Marquez ML, Hofmann AF, Xia Y, Steinbach JH, Ton-Nu H-T, Lillienau J, Angellotti MA, Schmassmann A (1991) *Gastroenterology* 100:212–221.
35. Amuro Y, Yamade W, Yamamoto T, Kudo K, Fujikura M, Maebo A, Hada T, Hoigashino K (1986) *Biochim Biophys Acta* 879:362–368.
36. Marschall HU, Oppermann UC, Svensson S, Nordling E, Persson B, Hooq JO, Jornvall H (2000) *Hepatology* 31:990–996.
37. Beuers U, Fischer S, Spengler U, Paumgartner G (1991) *J Hepatol* 13:97–103.
38. Schwarz M, Russell DW, Dietschy JM, Turley SD (1998) *J Lipid Res* 39:1833–1843.
39. Roda A, Hofmann AF, Mysels KJ (1983) *J Biol Chem* 258:6362–6370.
40. Sambrook J, Russell DW (2001) *Molecular Cloning: A Laboratory Manual* (Cold Spring Harbor Lab Press, Plainview, NY).
41. Mansour SL, Thomas KR, Capecchi MR (1988) *Nature* 336:348–352.
42. Turley SD, Daggy BP, Dietschy JM (1994) *Gastroenterology* 107:444–452.
43. Yokode M, Hammer RE, Ishibashi S, Brown MS, Goldstein JL (1990) *Science* 250:1273–1275.
44. Li-Hawkins J, Lund EG, Turley SD, Russell DW (2000) *J Biol Chem* 275:16536–16542.
45. Setchell KD, Street JM (1987) *Semin Liver Dis* 7:85–99.
46. Lawson AM, Setchell KDR (1988) in *The Bile Acids: Chemistry, Physiology, and Metabolism*, eds Setchell KDR, Kritchevsky D, Nair PP (Plenum, New York), pp 167–267.

BIOCHEMISTRY